

## Article

# Comparing the Structural and Physicochemical Properties of Highland Barley $\beta$ -Glucan from Different Sources: A Focus on Color

Ping Yu <sup>1,2,3</sup>, Xuemin Kang <sup>1,2,3</sup>, Pengfei Liu <sup>1,2,3</sup>, Zhengzong Wu <sup>1,2,3</sup> , Yue Cheng <sup>1,2,3</sup>, Bo Cui <sup>1,2,3,\*</sup> and Wei Gao <sup>1,2,3,\*</sup>

- <sup>1</sup> Shandong Key Laboratory of Healthy Food Resources Exploration and Creation, School of Food Sciences and Engineering, Qilu University of Technology, Shandong Academy of Sciences, Daxue Road, Changqing District, Jinan 250353, China; chemingmou@163.com (P.Y.); 15689408577@163.com (X.K.); zxliupf@163.com (P.L.); wzzqllu@hotmail.com (Z.W.); cylj144323@163.com (Y.C.)
- <sup>2</sup> State Key Laboratory of Biobased Material and Green Papermaking, Qilu University of Technology, Shandong Academy of Sciences, Daxue Road, Changqing District, Jinan 250353, China
- <sup>3</sup> School of Food Science and Engineering, Qilu University of Technology, Shandong Academy of Sciences, Daxue Road, Changqing District, Jinan 250353, China
- \* Correspondence: cuibopaper@163.com (B.C.); gaowei88666@163.com (W.G.)

**Abstract:** Herein,  $\beta$ -glucan (BG) was extracted from different colored varieties of highland barley (HB, *Hordeum vulgare*), defined as BBG, WBG, and LBG depending on the colors of black, white, and blue and their molecular structure and physicochemical properties were investigated through a series of technical methods. The high-performance anion-exchange chromatography (HPAEC) results indicated the extracted BBG, LBG, and WBG mainly comprised glucose regardless of color. The molecular weight ( $M_w$ ) of BBG, LBG, and WBG were 55.87 kDa, 65.19 kDa, and 81.59 kDa, respectively. 4-Glc(p), 3-Glc(p), and t-Glc(p) accounted for a larger proportion (>90%) of the total methylated residues according to gas chromatography–mass spectrometry (GC-MS) analysis. Additionally, Fourier transform infrared (FT-IR) spectroscopy revealed that the  $\beta$ -linkage of LBG had a greater capacity to develop stronger hydrogen bonds, due to the absence of 3,4-Glc(p). Among them, LBG had a low particle size distribution and a high shear viscosity, showing obvious round aggregates on its surface. Meanwhile, BBG presented a high peak viscosity (PV) and thermal stability. Based on the differences in their molecular structure, it could be concluded that there were different physicochemical properties among BBG, LBG, and WBG.

**Keywords:** highland barley;  $\beta$ -glucan; molecular structure; physicochemical properties



Academic Editor: Sean X Liu

Received: 13 December 2024

Revised: 9 January 2025

Accepted: 14 January 2025

Published: 18 January 2025

**Citation:** Yu, P.; Kang, X.; Liu, P.; Wu, Z.; Cheng, Y.; Cui, B.; Gao, W. Comparing the Structural and Physicochemical Properties of Highland Barley  $\beta$ -Glucan from Different Sources: A Focus on Color. *Foods* **2025**, *14*, 316. <https://doi.org/10.3390/foods14020316>

**Copyright:** © 2025 by the authors. Licensee MDPI, Basel, Switzerland. This article is an open access article distributed under the terms and conditions of the Creative Commons Attribution (CC BY) license (<https://creativecommons.org/licenses/by/4.0/>).

## 1. Introduction

$\beta$ -glucan is an important natural dietary fiber that is found in plants and microorganisms from natural sources such as grains, fungi, bacteria, and algae [1,2]. The intake of  $\beta$ -glucan can increase the viscosity of the digestive fluid in the gastrointestinal tract, extend the emptying time of the stomach, reduce the digestibility of starch, promote insulin secretion, and reduce the absorption rate of glucose, thereby leading to the inhibition and prevention of diabetes. Moreover,  $\beta$ -glucan is recognized as a hypocholesterolemic compound that can lower cholesterol and low-density lipoprotein (LDL) levels [3–5].

For the past several decades, there has been a general consensus that grain  $\beta$ -glucan is made up of mixed linkage (1,3) (1,4)  $\beta$ -D-glucose units. Nevertheless, the molecular structure and nutritional efficacy of  $\beta$ -glucan from different sources vary remarkably [2,6–10].

In particular, grain-derived  $\beta$ -glucan is a kind of non-starch polysaccharide existing in the endosperm and cell wall, which has attracted increasing attention due to its special physiological activity and medicinal value. In a previous study, cereal  $\beta$ -glucan showed prebiotic potential via microencapsulation with probiotics, which could provide better protective effects during gastrointestinal digestion [11]. Furthermore, there have been wide applications of cereal  $\beta$ -glucan, which can bind to proteins through more exposure sites in protein-based products, resulting in the formation of stronger three-dimensional gel networks and thereby improving the stability of protein gels [12].

The  $\beta$ -glucan content of highland barley (HB) is far greater than that of other grain crops [12]. In addition,  $\beta$ -glucan extracted from HB can interact with proteins through non-covalent bonds such as hydrogen bonding and electrostatic interactions, leading to the formation of a stronger three-dimensional gel network, which further promotes its application in the food industry [12,13]. The mechanical and barrier properties of highland barley  $\beta$ -glucan (HBBG) film have been enhanced through the incorporation of highland barley prolamin (HBP), resulting in the formation of hydrogen bonds between HBBG and HBP [14]. Both the fine structure and functional characteristics of  $\beta$ -glucan are also determined by the species, genetics, and growing conditions of HB [15]. Furthermore, it should be noted that there are many varieties of HB, which can be mainly divided into white, black, and blue according to their color [16]. Li et al. [17] found that the  $\beta$ -glucan extracted from the HB core had a higher  $M_w$  than that extracted from the HB outer bran, showing better foam stability and emulsifying properties. Colored (black and blue) HB varieties showed higher antioxidant, neuroprotective, hypoglycemic, and hypolipidemic properties than white HB [16]. Wang et al. [18] have also reported that colored HB contains a high amount of functional constituents, making it suitable for use in the functional food industry. Therefore, there is no doubt that  $\beta$ -glucans extracted from different colored HB varieties exhibit different molecular and physicochemical characteristics. However, limited investigations on the fine structure and physicochemical properties of  $\beta$ -glucans extracted from different colored HB varieties have been reported.

The main objective of this study was to extract  $\beta$ -glucan from different colored varieties of HB and investigate its molecular structure through a series of technical methods, including high-performance anion-exchange chromatography (HPAEC), size-exclusion chromatography (SEC) equipped with refractive index (RI) and multi-angle laser light-scattering (MALLS) detectors, X-ray diffraction (XRD) and Fourier transform infrared (FT-IR) spectroscopy. In addition, the physicochemical properties of the extracted  $\beta$ -glucans were evaluated via scanning electron microscopy (SEM), rapid viscosity analysis (RVA), and thermal stability analysis (TGA). The relevant fluid viscosity results could provide a theoretical basis facilitating the precise processing and high-value utilization (cosmetics and drug delivery) of  $\beta$ -glucan.

## 2. Materials and Methods

### 2.1. Materials

HB seeds of different colors (black, white, and blue) were provided by Qinghai Lanke Agriculture and Animal Husbandry Technology Co., Ltd. (Qinghai, China). High temperature resistant  $\alpha$ -amylase (BR, 4000 U/g), amyloglucosidase (deriving from *Aspergillus niger*, BR, 100,000 U/g), pancreatin (BR, 4000 U/g), and the dialysis bag (molecular weight cut-off of 3500 Da) were purchased from Yuanye Bio-Technology Co., Ltd. (Shanghai, China). The  $\beta$ -glucan Assay Kit (Mixed Linkage) was purchased from Megazyme International LTD, Bray, Co. Wicklow, Ireland. Ethanol (95%, *v/v*) was provided by Fuyu Fine Chemical Co., Ltd. (Tianjin, China). Methanol, trifluoroacetic acid, acetic acid, and dichloromethane were purchased from ANPEL Laboratory Technologies (Shanghai) Inc. (Shanghai, China).

Monosaccharide standards (fucose, rhamnose, arabinose, galactose, glucose, xylose, mannose, fructose, ribose, galacturonic acid, glucuronic acid, mannuronic acid, and guluronic acid), sodium hydroxide, sodium acetate trihydrate, dimethyl sulfoxide, sodium borodeuteride and acetic anhydride were purchased from Sigma-Aldrich Chemical Co. (St. Louis, MO, USA). Sodium nitrate (AR grade) was purchased from Sinopharm Group Co., Ltd. (Shanghai, China).

## 2.2. Pretreatment of HB Samples

HB was ground using a laboratory mill and then sieved through a 0.50 mm screen to obtain HB flour. The HB flour (50 g) was then suspended in 500 mL of aqueous ethanol and stirred under backflow for 4 h. The mixture was filtered to obtain the precipitate and heated to a constant weight in an oven at 60 °C. The obtained samples were crushed for further analysis.

## 2.3. Extraction and Quantification of $\beta$ -Glucan

The extraction of  $\beta$ -glucan was determined using a previously reported method with minor modifications [11,19]. Please refer to the Supplementary Materials.

The  $\beta$ -glucan crude extract was defined as BBG, WBG, and LBG, depending on the colors of black, white, and blue, respectively. All extraction processes were repeated three times. Images of the  $\beta$ -glucan samples are presented in Figure 1.

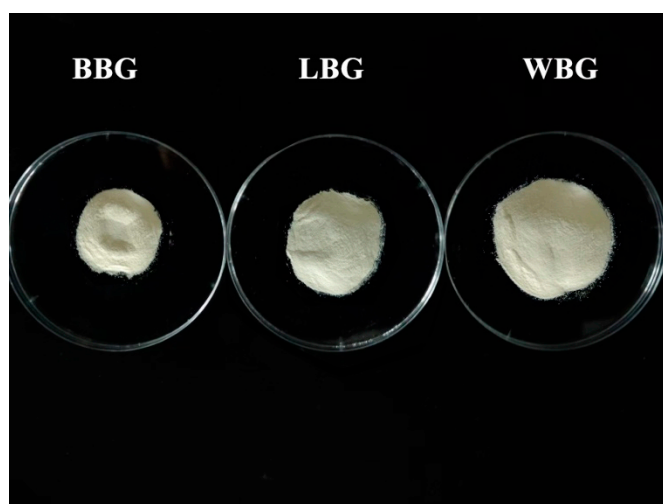


**Figure 1.** Images of  $\beta$ -glucan extracting from different colors of highland barley (BBG indicates black highland barley  $\beta$ -glucan; LBG indicates blue highland barley  $\beta$ -glucan; WBG indicates white highland barley  $\beta$ -glucan).

## 2.4. Purity, Moisture Content (MC) and Color Variation in $\beta$ -Glucan

The purity of BBG, WBG, and LBG was determined using the Congo red method [15,20], while the water content and color variation in samples were analyzed following our reported method [21]. Please refer to the Supplementary Materials.

## 2.5. Molecular Structure Analysis

### 2.5.1. Monosaccharide Composition

The monosaccharide composition analysis of BBG, WBG, and LBG was determined according to the method described by Bai et al. [19]. Please refer to the Supplementary Materials.

### 2.5.2. Methylation Analysis

The methylation analysis of BBG, WBG, and LBG was analyzed following the method described by Li et al. [22]. Please refer to the Supplementary Materials.

### 2.5.3. Molecular Weight Determination

The molecular weight of BBG, WBG, and LBG was measured following the method described by Du et al. [23]. Please refer to the Supplementary Materials.

### 2.5.4. XRD

The crystalline structure and relative crystallinity of  $\beta$ -glucan samples were examined using a previously reported method [24]. Please refer to the Supplementary Materials.

### 2.5.5. FT-IR

The FT-IR spectra of the  $\beta$ -glucan sample were obtained following our previous method [24]. Please refer to the Supplementary Materials.

## 2.6. Particle Morphology Analysis

### 2.6.1. SEM

The  $\beta$ -glucan samples were fixed on a conductive carbon tape and coated with Au/Pd. Subsequently, they were observed through a Hitachi scanning electron microscope (Tokyo, Japan) at a voltage of 5 kV [25].

### 2.6.2. Particle Size Distribution Determination

The particle size analysis of  $\beta$ -glucan was performed using a Microtrac MRB equipped with a dynamic light scattering system (Microtrac Inc., Montgomeryville, PA, USA) with a refractive index of 1.67 and a focusing time of 30 s. At room temperature, the samples were dispersed uniformly into a flowing aqueous cuvette. The test was initiated when the sample concentration reached the standard concentration.

## 2.7. Physicochemical Properties

### 2.7.1. RVA

The viscosity curve of the  $\beta$ -glucan samples was measured following the standard 13 min program [26]. Details can be found in the Supplementary Materials.

### 2.7.2. Rheological Measurements

The dynamic rheological properties of  $\beta$ -glucan were analyzed according to the method of Iqbal et al. [27] with modifications. Details can be found in the Supplementary Materials.

### 2.7.3. TGA

The thermogravimetric analysis of the  $\beta$ -glucan samples was performed according to our previous method [26].

## 2.8. Statistical Analyses

All experimental data were evaluated by running the ANOVA procedure and employing Duncan's multiple range test ( $p < 0.05$ ).

## 3. Results and Discussion

### 3.1. Characteristics of $\beta$ -Glucan

The extractability, purity, and MC of BBG, LBG, and WBG are shown in Table 1. The  $\beta$ -glucan extractability of black, blue, and white highland barley varieties was 4.94%,

3.32%, and 4.47%, respectively. Moreover, black highland barley exhibited the highest extractability of  $\beta$ -glucan. These results correspond with the findings published by Bai et al. [19]. The purity of BBG, LBG, and WBG was all greater than 80%, while the MC values of all the  $\beta$ -glucan samples were less than 12%, indicating the extraction method in this study was effective.

**Table 1.** Extractability, purity, and MC of BBG, LBG, and WBG (BBG indicates black highland barley  $\beta$ -glucan; LBG indicates blue highland barley  $\beta$ -glucan; WBG indicates white highland barley  $\beta$ -glucan).

Sample	Extractability/%	Purity/%	MC (%)
BBG	4.94 $\pm$ 0.09 <sup>b</sup>	89.06 $\pm$ 1.99 <sup>b</sup>	10.91 $\pm$ 0.29 <sup>a</sup>
WBG	4.47 $\pm$ 0.18 <sup>b</sup>	82.37 $\pm$ 1.23 <sup>a</sup>	11.84 $\pm$ 0.09 <sup>b</sup>
LBG	3.32 $\pm$ 0.24 <sup>a</sup>	83.69 $\pm$ 1.74 <sup>a</sup>	11.85 $\pm$ 0.22 <sup>b</sup>

The values correspond to the mean  $\pm$  standard deviation ( $n = 3$ ). Different letters in the same column indicate significant differences ( $p < 0.05$ ).

The color variation in BBG, LBG, and WBG is shown in Table 2. L\* (0 (black) to 100 (white)), a\* (−80 (greenness) to 100 (redness)) and b\* (−80 (blueness) to 70 (yellowness)) reflect whiteness, redness, and yellowness, respectively, while  $\Delta E$  indicates the color difference [21]. There were significant differences among all the  $\beta$ -glucan samples for b\* (ranging from 9.37 to 11.60) and  $\Delta E$  values, which might be closely related to appearance and consumer acceptance. Interestingly, LBG had the highest L\* value of 83.38, indicating that it showed an opaque white color.

**Table 2.** Color variation in BBG, LBG, and WBG (BBG indicates black highland barley  $\beta$ -glucan; LBG indicates blue highland barley  $\beta$ -glucan; WBG indicates white highland barley  $\beta$ -glucan).

Sample	L*	a*	b*	$\Delta E^*$
BBG	72.40 $\pm$ 0.07 <sup>b</sup>	1.94 $\pm$ 0.01 <sup>ab</sup>	10.72 $\pm$ 0.01 <sup>c</sup>	17.31 $\pm$ 0.08 <sup>a</sup>
WBG	82.36 $\pm$ 1.76 <sup>a</sup>	3.29 $\pm$ 0.75 <sup>a</sup>	11.60 $\pm$ 1.05 <sup>a</sup>	7.11 $\pm$ 0.16 <sup>c</sup>
LBG	83.38 $\pm$ 0.01 <sup>a</sup>	1.41 $\pm$ 0.04 <sup>b</sup>	9.37 $\pm$ 0.09 <sup>b</sup>	6.25 $\pm$ 0.01 <sup>b</sup>

The values correspond to the mean  $\pm$  standard deviation ( $n = 3$ ). Different letters in the same column indicate significant differences ( $p < 0.05$ ).

### 3.2. Molecular Structure Analysis

#### 3.2.1. Monosaccharide Composition and Methylation Analysis

The monosaccharide composition chromatograms of the standards and the BBG, LBG, and WBG samples are shown in Figure 2. Furthermore, the percentage of the monosaccharides is displayed in Table 3. Monosaccharide standards (fucose, rhamnose, arabinose, galactose, glucose, xylose, mannose, fructose, ribose, galacturonic acid, glucuronic acid, mannuronic acid, and guluronic acid) were employed to identify and measure the corresponding peaks in the monosaccharide composition analysis of different colors of HB. There were three peaks in the elution curves of BBG, LBG, and WBG shown on the standard substance graph, which were related to arabinose, glucose, and xylose. As expected, the extracted BBG, LBG, and WBG mainly comprised glucose, regardless of the color. The other impurities were probably the source of the trace levels of xylose and arabinose [19].

According to Table 4, there were seven different linkage patterns in the GC-MS spectrum of methylated alditol acetates obtained from BBG and WBG. Meanwhile, LBG had six linkage patterns. Among the samples, 4-Glc(p), 3-Glc(p), and t-Glc(p) accounted for a larger proportion (>90%) of the total methylated residues, indicating that the extracted  $\beta$ -glucan mainly comprised three forms of sugar linkages. Additionally, there was no 3,4-Glc(p) in LBG.

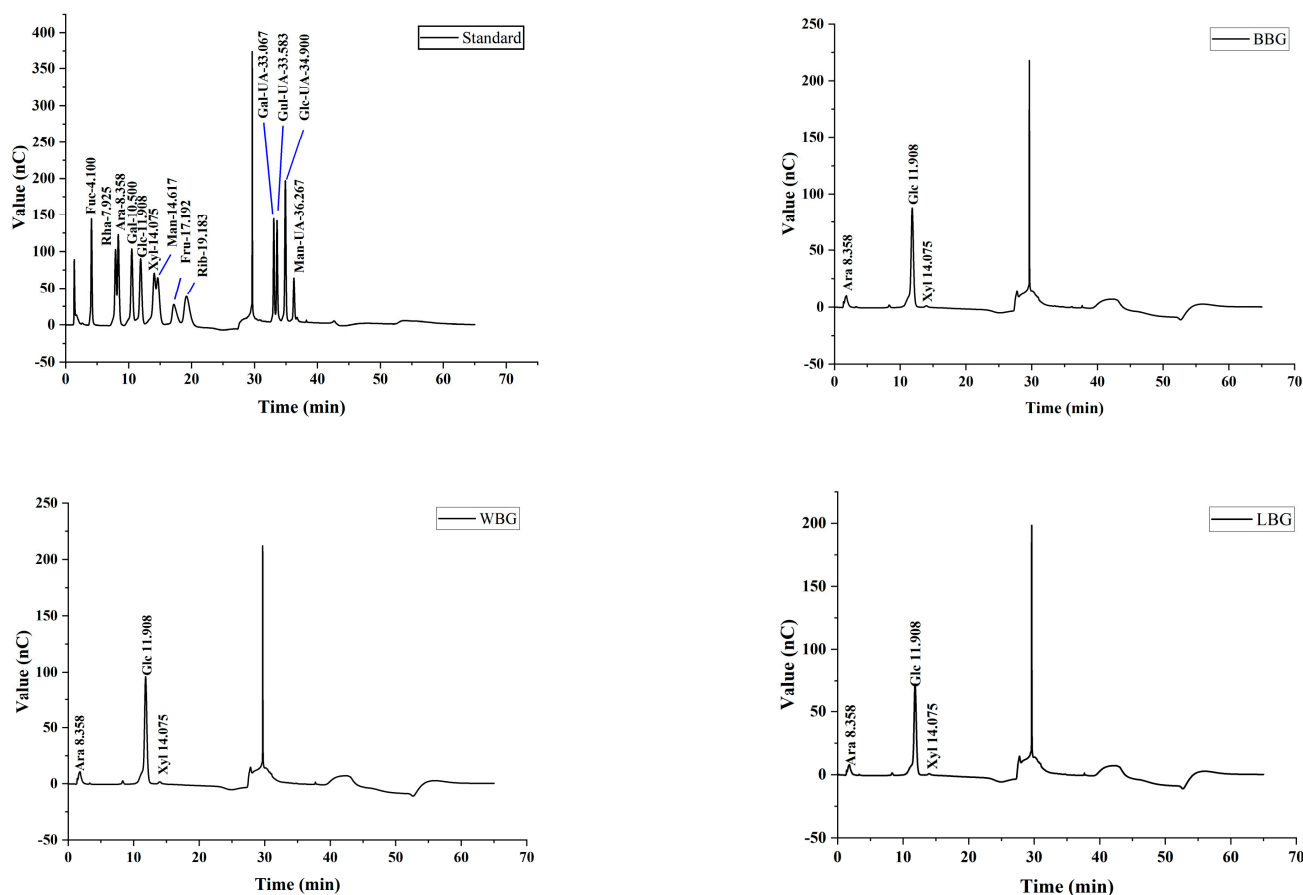


**Figure 2.** Monosaccharide composition chromatograms of standards, BBG, LBG and WBG samples (BBG indicates black highland barley β-glucan; LBG indicates blue highland barley β-glucan; WBG indicates white highland barley β-glucan).

**Table 3.** Monosaccharide composition (molar ratio/%) of BBG, WBG, and LBG (BBG indicates black highland barley β-glucan; LBG indicates blue highland barley β-glucan; WBG indicates white highland barley β-glucan).

Sample	Arabinose	Glucose	Xylose
BBG	1.47%	96.75%	1.78%
WBG	1.52%	96.65%	1.83%
LBG	1.71%	95.97%	2.32%

**Table 4.** Methylation analysis of BBG, LBG, and WBG (BBG indicates black highland barley β-glucan; LBG indicates blue highland barley β-glucan; WBG indicates white highland barley β-glucan).

Sample	Linkage Patterns	Derivative Name	RT	Molar Ratios (%)
BBG	t-Ara(f)	1,4-di-O-acetyl-2,3,5-tri-O-methyl arabinitol	6.001	1.61
	t-Glc(p)	1,5-di-O-acetyl-2,3,4,6-tetra-O-methyl glucitol	8.800	6.97
	4-Xyl(p)	1,4,5-tri-O-acetyl-2,3-di-O-methyl xylitol	11.409	1.25
	3-Glc(p)	1,3,5-tri-O-acetyl-2,4,6-tri-O-methyl glucitol	11.976	17.37
	4-Glc(p)	1,4,5-tri-O-acetyl-2,3,6-tri-O-methyl glucitol	13.918	66.39
	3,4-Glc(p)	1,3,4,5-tetra-O-acetyl-2,6-di-O-methyl glucitol	16.064	1.42
	4,6-Glc(p)	1,4,5,6-tetra-O-acetyl-2,3-di-O-methyl glucitol	18.153	4.99

Table 4. Cont.

Sample	Linkage Patterns	Derivative Name	RT	Molar Ratios (%)
WBG	t-Ara(f)	1,4-di-O-acetyl-2,3,5-tri-O-methyl arabinitol	5.987	1.59
	t-Glc(p)	1,5-di-O-acetyl-2,3,4,6-tetra-O-methyl glucitol	8.779	6.19
	4-Xyl(p)	1,4,5-tri-O-acetyl-2,3-di-O-methyl xylitol	11.391	1.30
	3-Glc(p)	1,3,5-tri-O-acetyl-2,4,6-tri-O-methyl glucitol	11.980	20.94
	4-Glc(p)	1,4,5-tri-O-acetyl-2,3,6-tri-O-methyl glucitol	13.961	64.50
	3,4-Glc(p)	1,3,4,5-tetra-O-acetyl-2,6-di-O-methyl glucitol	16.050	1.44
	4,6-Glc(p)	1,4,5,6-tetra-O-acetyl-2,3-di-O-methyl glucitol	18.138	4.04
LBG	t-Ara(f)	1,4-di-O-acetyl-2,3,5-tri-O-methyl arabinitol	5.983	1.32
	t-Glc(p)	1,5-di-O-acetyl-2,3,4,6-tetra-O-methyl glucitol	8.779	6.04
	4-Xyl(p)	1,4,5-tri-O-acetyl-2,3-di-O-methyl xylitol	11.391	1.17
	3-Glc(p)	1,3,5-tri-O-acetyl-2,4,6-tri-O-methyl glucitol	11.976	22.23
	4-Glc(p)	1,4,5-tri-O-acetyl-2,3,6-tri-O-methyl glucitol	13.957	66.87
	4,6-Glc(p)	1,4,5,6-tetra-O-acetyl-2,3-di-O-methyl glucitol	18.142	2.37

### 3.2.2. Molecular Weight Distribution Analysis

The multi-angle laser light scattering (LS), refractive index (RI), and molar mass curves of BBG, LBG, and WBG are presented in Figure 3. There were two peaks that emerged within the elution time from 10 to 30 min in the LS profiles of BBG and WBG, while the LS profiles of LBG exhibited three peaks, suggesting the presence of larger aggregates of  $\beta$ -glucan in the  $\text{NaNO}_3$  solution, especially for the LBG sample [28]. Moreover, peak II that emerged at approximately 20 min could be due to the flexible individual chains of  $\beta$ -glucan [29]. These findings could demonstrate that the samples were unevenly dispersed in the  $\text{NaNO}_3$  solution through the presence of two forms of larger aggregates and flexible individual chains. The disappearance of peak II in the BBG and WBG samples might be related to the formation of intermolecular interaction among the side chains of  $\beta$ -glucan, thus forming a loose network [28].

There were three peaks of RI signal in the BBG, LBG, and WBG curves, but these peaks emerged at different elution times and in different peak areas. In addition, the solvent peak of the mobile phase ( $\text{NaNO}_3$  solution) emerged at nearly 37 min. As shown in Table 5, the molecular weight ( $M_w$ ) of BBG was 55.87 kDa, which was lower than that of LBG (65.19 kDa) and WBG (81.59 kDa). It was also previously reported that the  $M_w$  (648.2 kDa) of  $\beta$ -glucan extracted from the inner fraction of HB was higher than that extracted from the HB outer bran (58.59 kDa) [17]. Moreover, the reduced polydispersity ( $M_w/M_n$ ) values of LBG, BBG, and WBG were 2.83, 2.36, and 2.23, respectively, indicating a more uniform molecule distribution of  $\beta$ -glucan [19]. Additionally, the findings illustrated that the  $\beta$ -glucan extracted from different colored varieties of highland barley showed different sizes and conformations [30].

**Table 5.** Analysis of molecular weight data of three  $\beta$ -glucans (BBG indicates black highland barley  $\beta$ -glucan; LBG indicates blue highland barley  $\beta$ -glucan; WBG indicates white highland barley  $\beta$ -glucan).

Sample	$M_n$ (kDa)	$M_w$ (kDa)	Polydispersity ( $M_w/M_n$ )
BBG	24.35 $\pm$ 0.17 <sup>b</sup>	55.87 $\pm$ 0.24 <sup>a</sup>	2.36 $\pm$ 0.05 <sup>a</sup>
WBG	36.75 $\pm$ 0.15 <sup>c</sup>	81.59 $\pm$ 0.18 <sup>c</sup>	2.23 $\pm$ 0.07 <sup>a</sup>
LBG	22.54 $\pm$ 0.13 <sup>a</sup>	65.19 $\pm$ 0.08 <sup>b</sup>	2.83 $\pm$ 0.09 <sup>b</sup>

The values correspond to the mean  $\pm$  standard deviation ( $n = 3$ ). Different letters in the same column indicate significant differences ( $p < 0.05$ ).

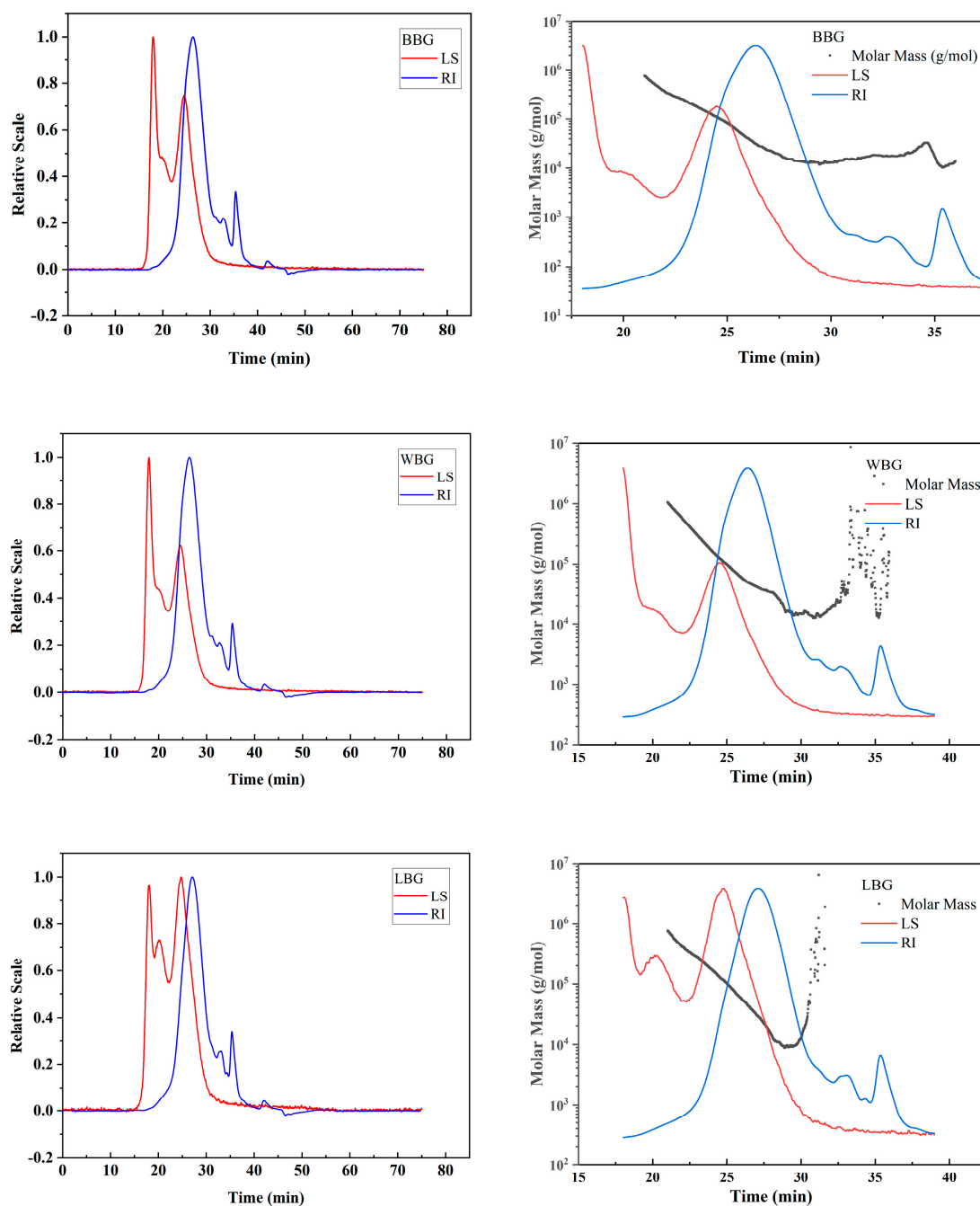


**Figure 3.** The profiles of molar mass/RI/LS signals versus elution time (min) of BBG, LBG, and WBG (BBG indicates black highland barley  $\beta$ -glucan; LBG indicates blue highland barley  $\beta$ -glucan; WBG indicates white highland barley  $\beta$ -glucan).

### 3.2.3. XRD Analysis

The XRD patterns and relative crystallinity (RC) of BBG, LBG, and WBG are shown in Figure 4. It is evident that the diffraction patterns of BBG, WBG, and LBG all exhibited a wide peak at  $2\theta = 20^\circ$ , indicating the formation of the relatively regular crystalline and amorphous forms during the extraction and purification process [29]. A similar result was also observed by Bai et al. [19], who reported that there was a broader peak at  $2\theta = 20^\circ$  in the crystalline region of  $\beta$ -glucan after heat fluidization and microwave treatments. In fact, the crystalline structure of the  $\beta$ -glucan samples was significantly affected by the extraction method. The barley  $\beta$ -glucan extracted assisting with the high-speed centrifugal vortex method showed a narrower peak than the control sample [31]. Furthermore, new weak

peaks at approximately  $2\theta = 13^\circ$  were observed for BBG, WBG, and LBG, leading to the conclusion that there were multiple crystal-like structures and lattice types in the crystalline portion [19]. It should be noted that the RC values of all samples ranged from 0.48 to 0.52%, which were much lower than that of hull-less barley  $\beta$ -glucan (RC = 28.37%) with a high  $M_w$  (3100 kDa) [32]. Li et al. [32] concluded that a high molecular weight and a dense micrographic network contributed to the formation of crystalline structures.

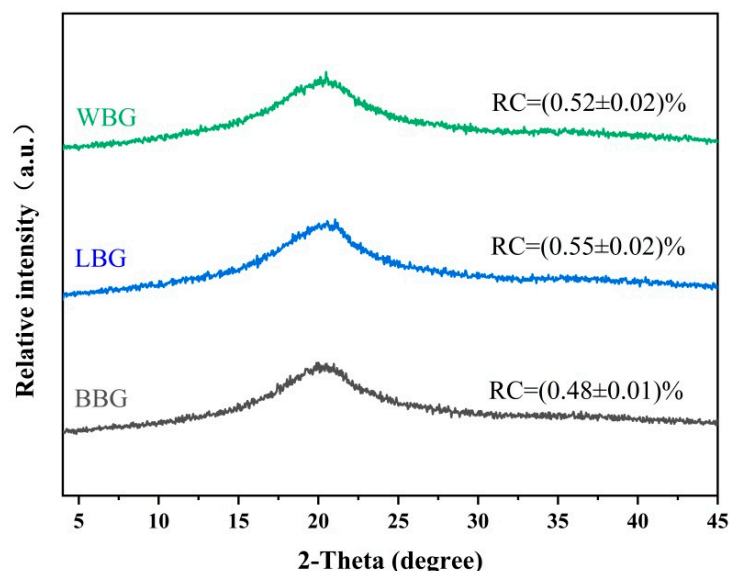


**Figure 4.** XRD spectrum of BBG, LBG, and WBG (BBG indicates black highland barley  $\beta$ -glucan; LBG indicates blue highland barley  $\beta$ -glucan; WBG indicates white highland barley  $\beta$ -glucan).

#### 3.2.4. FT-IR Analysis

The FT-IR spectra curves of BBG, LBG, and WBG are shown in Figure 5. All the sample spectra exhibited a similar trend, suggesting that there were little changes in the functional groups of  $\beta$ -glucan among the different colored HB varieties. The peaks in the region of  $3343\text{--}3325\text{ cm}^{-1}$  were due to the asymmetric stretching vibration of hydroxyl O-H resulting from the interactions between glycosidic linkages within the polysaccharide chain [33], while the peaks around  $2881\text{ cm}^{-1}$  were attributed to C-H stretching vibration on saturated carbons [34]. Furthermore, it was observed that the characteristic peaks representing hydroxyl O-H of BBG, LBG, and WBG emerged at  $3343.3\text{ cm}^{-1}$ ,  $3325.6\text{ cm}^{-1}$ , and  $3322.7\text{ cm}^{-1}$ , respectively. According to the harmonic oscillator model [35], the inter- and intra-molecular hydrogen bonding interactions between hydroxyl groups within the polysaccharide chain were in the following order: WBG > LBG > BBG. Meanwhile, the chemical shift value around  $1654.2\text{ cm}^{-1}$  was due to the asymmetric stretching of C=O, which has also been reported to be due to the binding of  $\beta$ -glucan to water [36]. Additionally, the vibration peaks between  $1017.9$  and  $1155.4\text{ cm}^{-1}$  were related to the C-O-C stretching of glycosidic linkages [37]. Interestingly, the intensity of these two peaks was in the following order: LBG > WBG > BBG, which indicated that more molecular chains of  $\beta$ -glucan were broken depending on the color during the heat extraction processing. This result could also be explained by the harmonic oscillator model mentioned above, which proposes that molecular interaction is enhanced with a decrease in the peak frequency. Furthermore, the absorption peak at approximately  $893.6\text{ cm}^{-1}$  was associated with the stretching vibrations of the  $\beta$ -linked glycosidic bond [19,38]. Due to the absence of 3,4-Glc(p), the strongest intensity of this characteristic “anomeric region” was observed in LBG, indicating that the  $\beta$ -linkage of pyranose obtained from blue highland barley had more opportunity to form stronger hydrogen bonds [39,40].

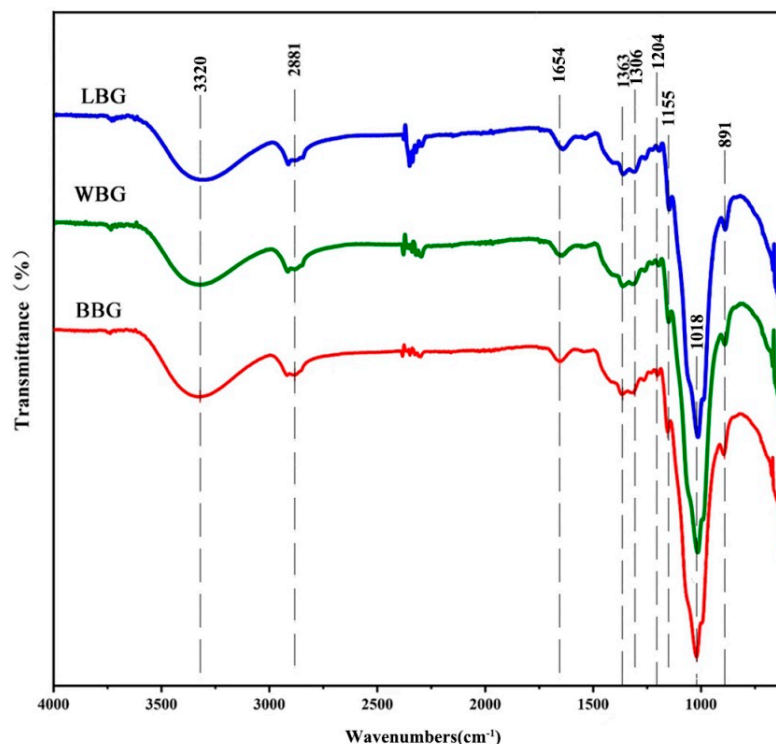


**Figure 5.** FT-IR spectrum of BBG, LBG, and WBG (BBG indicates black highland barley  $\beta$ -glucan; LBG indicates blue highland barley  $\beta$ -glucan; WBG indicates white highland barley  $\beta$ -glucan).

### 3.3. Particle Morphology Analysis of $\beta$ -Glucan

#### 3.3.1. Morphology Observation

The SEM morphologies of BBG, LBG, and WBG are shown in Figure 6. Generally, all the  $\beta$ -glucan samples exhibited rough surfaces, which showed spheroidal aggregates of different sizes. This may be due to the greater molecular weight of  $\beta$ -glucans extracted by means of hot water without seriously damaging its molecular structure. Similar results have been proposed by Dong et al. [37], who found that thermal processing (steaming or microwave) could hinder the aggregation of oat  $\beta$ -glucan. As shown in Figure 6, it can also be concluded that there were many obvious round aggregates in LBG, while WBG and BBG were mostly composed of large and compact aggregates. Cory et al. [41] suggested that it may also be related to the growing environment and gene regulation. Ma et al. [42] reported that there were compact aggregated clusters with honeycomb-like structures in yeast  $\beta$ -glucan.

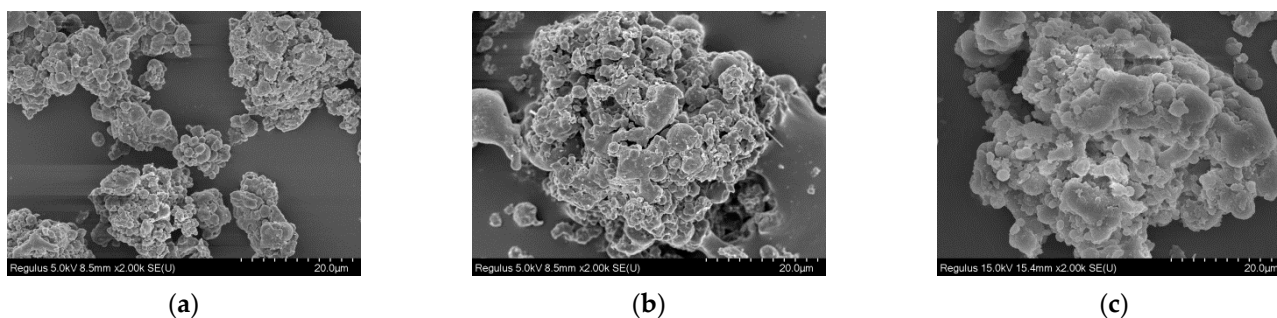


**Figure 6.** Surface morphology of BBG (a), LBG (b), WBG (c) with a magnification of 2000 (BBG indicates black highland barley  $\beta$ -glucan; LBG indicates blue highland barley  $\beta$ -glucan; WBG indicates white highland barley  $\beta$ -glucan).

### 3.3.2. Particle Size Distribution Determination

The particle size distribution curves and parameters ( $D(4,3)$ ,  $D(3,2)$ ,  $D_{10}$ ,  $D_{50}$ , and  $D_{90}$ ) of the BBG, WBG, and LBG samples are shown in Figure 7 and Table 6, respectively. Particle size distribution is an important factor affecting the aggregation state and conformation of  $\beta$ -glucan [43]. Specifically, the  $D_{50}$  values of WBG, BBG, and LBG were 112.75  $\mu\text{m}$ , 112.15  $\mu\text{m}$ , and 87.93  $\mu\text{m}$ , respectively. The  $D(4,3)$  values of WBG, BBG, and LBG were in descending order with 130.60  $\mu\text{m}$ , 127.75  $\mu\text{m}$ , and 107.70  $\mu\text{m}$ , respectively. Meanwhile, the WBG, BBG, and LBG samples exhibited  $D(3,2)$  values of 55.94  $\mu\text{m}$ , 56.57  $\mu\text{m}$ , and 40.72  $\mu\text{m}$ , respectively. The closer the values of  $D(3,2)$  and  $D(4,3)$ , the more regular the shape of the sample particles; this means that the particle size distribution is more concentrated [44]. These results indicated that LBG provided the best dispersion in water, which was similar to the finding observed by SEM.

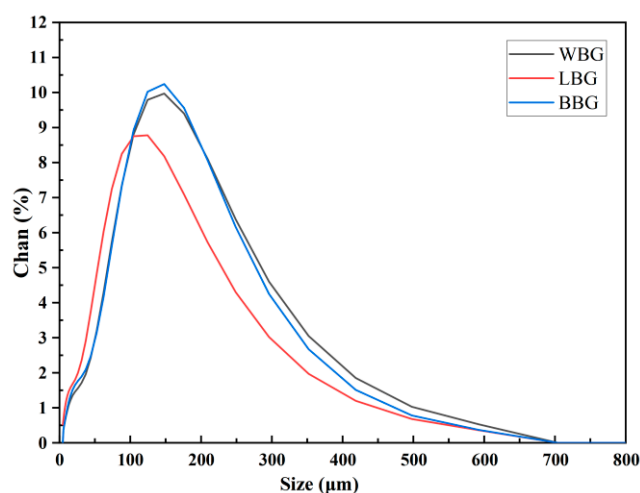


**Figure 7.** Particle-size distribution of BBG, LBG, and WBG (BBG indicates black highland barley  $\beta$ -glucan; LBG indicates blue highland barley  $\beta$ -glucan; WBG indicates white highland barley  $\beta$ -glucan).

**Table 6.** Particle size parameters of BBG, LBG, and WBG (BBG indicates black highland barley  $\beta$ -glucan; LBG indicates blue highland barley  $\beta$ -glucan; WBG indicates white highland barley  $\beta$ -glucan).

Sample	$D_{10}$ ( $\mu\text{m}$ )	$D_{50}$ ( $\mu\text{m}$ )	$D_{90}$ ( $\mu\text{m}$ )	$D(4,3)$ ( $\mu\text{m}$ )	$D(3,2)$ ( $\mu\text{m}$ )
BBG	24.90 $\pm$ 0.56 <sup>a</sup>	112.15 $\pm$ 0.55 <sup>a</sup>	244.15 $\pm$ 1.45 <sup>a</sup>	127.75 $\pm$ 0.05 <sup>a</sup>	56.57 $\pm$ 0.68 <sup>a</sup>
WBG	25.60 $\pm$ 1.02 <sup>a</sup>	112.75 $\pm$ 1.15 <sup>a</sup>	253.65 $\pm$ 4.15 <sup>a</sup>	130.60 $\pm$ 2.10 <sup>a</sup>	55.94 $\pm$ 2.09 <sup>a</sup>
LBG	17.21 $\pm$ 0.21 <sup>b</sup>	87.93 $\pm$ 0.16 <sup>b</sup>	220.1 $\pm$ 1.3 <sup>b</sup>	107.70 $\pm$ 0.60 <sup>b</sup>	40.72 $\pm$ 0.46 <sup>b</sup>

The values correspond to the mean  $\pm$  standard deviation ( $n = 3$ ). Different letters in the same column indicate significant differences ( $p < 0.05$ ).

### 3.4. Physicochemical Properties

#### 3.4.1. Rapid Viscosity Analysis (RVA)

The gelatinization performance of BBG, LBG, and WBG measured by RVA is shown in Figure 8. Meanwhile, the pasting parameters (pasting temperature, PT; peak viscosity, PV; trough viscosity, TV; final viscosity, FV; breakdown, BD; and setback, SB), reflecting the molecular structure evolution of  $\beta$ -glucan during the heating cycle, are presented in Table 7. The BBG and WBG samples displayed similar pasting profile shapes, which were distinctly different from that of LBG, thus indicating a significant change in their pasting parameters. Specifically, the highest PV value of 296.5 cP was observed in BBG, followed by WBG (295 cP) and LBG (183 cP). As shown in the thermal stability results, LBG showed

the strongest water-binding capacity among all the  $\beta$ -glucan samples, thus exhibiting a poor ability to form a network gel structure and a low PV value during the heating cycle. Correspondingly, the ability of the sample to swell and bind water was positively correlated with the gelatinization temperature [45]. Therefore, the PT values of BBG, WBG, and LBG were in the descending order of 73.38 °C, 72.95 °C, and 70.18 °C, respectively. Furthermore, the stability and degradation of the  $\beta$ -glucan paste during the heating–cooling cycle are reflected by the BD and SB values [46]. As shown in Table 7, LBG had the lowest BD and SB values of 78.5 and 170.5, respectively, indicating that the stability of LBG paste was higher than that of BBG and WBG pastes. Moreover, the paste viscosity was positively influenced by particle size [47]. These observations were also consistent with the particle size distribution results.

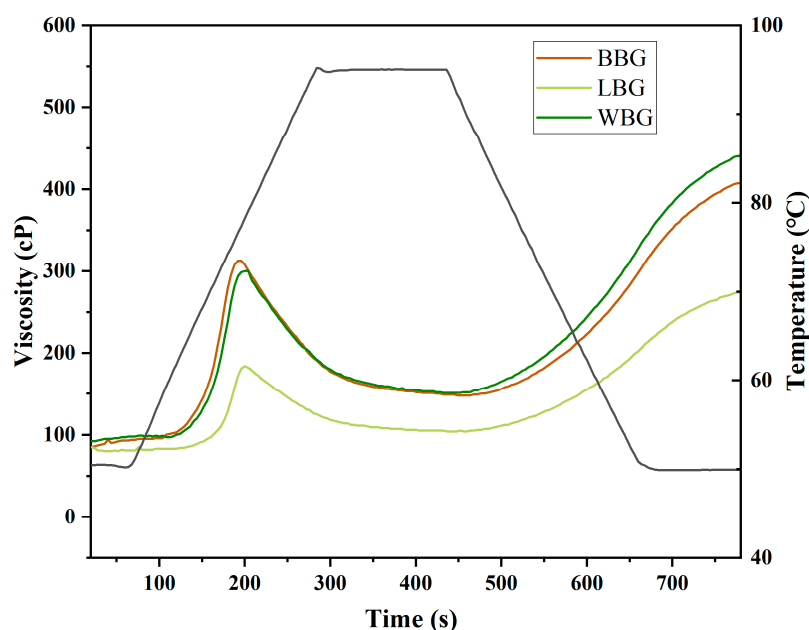


**Figure 8.** Rapid viscosity analysis of BBG, LBG, and WBG (BBG indicates black highland barley  $\beta$ -glucan; LBG indicates blue highland barley  $\beta$ -glucan; WBG indicates white highland barley  $\beta$ -glucan).

**Table 7.** Pasting properties of BBG, LBG, and WBG (BBG indicates black highland barley  $\beta$ -glucan; LBG indicates blue highland barley  $\beta$ -glucan; WBG indicates white highland barley  $\beta$ -glucan).

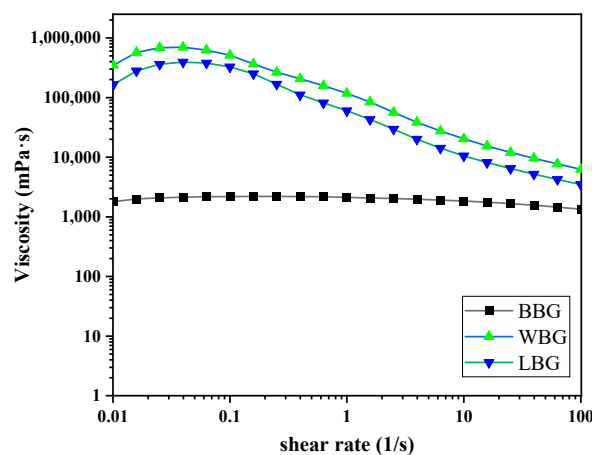
Sample	PV (cP)	TV (cP)	BD (cP)	FV (cP)	SB (cP)	PT (°C)
BBG	296.5 ± 4.95 <sup>b</sup>	147 ± 1.41 <sup>c</sup>	149.5 ± 3.54 <sup>c</sup>	399 ± 1.31 <sup>c</sup>	252 ± 2.9 <sup>c</sup>	73.38 ± 0.04 <sup>c</sup>
WBG	295 ± 2.46 <sup>b</sup>	142 ± 0.73 <sup>b</sup>	153 ± 0.73 <sup>b</sup>	399.5 ± 0.28 <sup>b</sup>	257.5 ± 0.55 <sup>b</sup>	72.95 ± 1.76 <sup>b</sup>
LBG	183 ± 1.41 <sup>a</sup>	104.5 ± 0.71 <sup>a</sup>	78.5 ± 2.12 <sup>a</sup>	275 ± 1.41 <sup>a</sup>	170.5 ± 0.71 <sup>a</sup>	70.18 ± 0.08 <sup>a</sup>

The values correspond to the mean ± standard deviation ( $n = 3$ ). Different letters in the same column indicate significant differences ( $p < 0.05$ ).

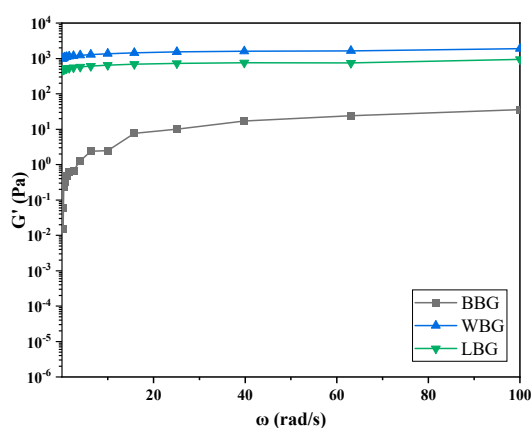
### 3.4.2. Rheological Measurements

The dynamic rheological data of BBG, WBG, and LBG are shown in Figure 9. The inter-chain relationships between polysaccharides can be understood through the observation of rheological behavior.  $\beta$ -glucan with a 4% concentration mainly manifests as intermolecular entanglement and gel formation in an aqueous solution [39]. In dynamic rheological behavior analysis, the storage modulus ( $G'$ ) characterizes the strength of the gel and the loss modulus ( $G''$ ) indicates the change in the viscosity of the sol, which could be employed to investigate the viscoelastic properties of mixed gel systems. The  $G'$  values of WBG and LBG were higher than the  $G''$  values, indicating that their fluids showed a weak gel

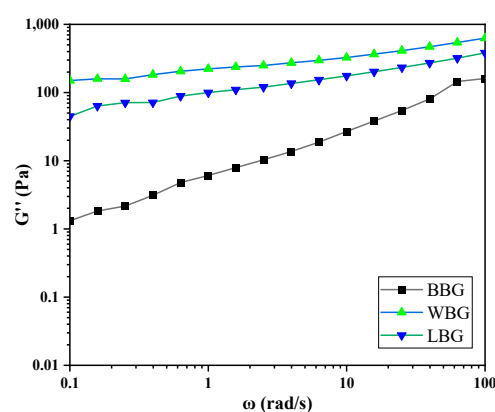
structure [48]. Interestingly, the  $G'$  value of the BBG fluid was lower than the  $G''$  value, which is a typical characteristic of an entangled viscoelastic liquid, indicating that it could be used in jam food systems with high viscosity maintenance requirements. In addition, both WBG and LBG had higher dynamic modulus ( $G'$  and  $G''$  values) than BBG, suggesting stronger viscoelastic behaviors. The gelation process of grain  $\beta$ -glucan was found to depend on the molar mass and aggregation state of  $\beta$ -glucan molecules.



(A)



(B)



(C)

**Figure 9.** Apparent viscosity (A) and dynamic rheological (B,C) curves of BBG, WBG, LBG (BBG indicates black highland barley  $\beta$ -glucan; LBG indicates blue highland barley  $\beta$ -glucan; WBG indicates white highland barley  $\beta$ -glucan).

As shown in Figure 9, the viscosity of WBG and LBG decreased significantly with increasing shear rate, exhibiting shear-thinning flow behavior, while the viscosity of BBG remained stable. Li et al. [49] concluded that this phenomenon was due to the same directional movement of  $\beta$ -glucan molecules and the destruction of molecular entanglement caused by strong shear action. The shear viscosity of  $\beta$ -glucan dispersion was related to the average molecular weight, concentration, and composition [50]. The WBG and LBG samples with a large molecular weight showed a higher shear viscosity than the BBG sample. This may be due to the stronger intermolecular interactions and the higher entanglement among molecular chains in the WBG and LBG samples with a high  $M_w$ . Similarly,  $\beta$ -glucan extracted from the HB core with a high  $M_w$  exhibited higher apparent viscosity than that extracted from the outer bran due to the stronger molecular chain entanglements [17]. Furthermore, the flow behavior index ( $n$ ) of the different samples was less than 1, indicating

that all samples were pseudoplastic fluids. The gel-like properties of high-molecular-weight  $\beta$ -glucan suggest potential applications in food processing, cosmetics, and drug delivery [51].

### 3.4.3. Thermal Property Measurement

The thermogravimetric (TG) and differential thermogravimetric (DTG) spectra of BBG, LBG, and WBG are shown in Figure 10. There were two distinct stages of weight loss shown in the curves of all samples. The DTG curve was derived from TGA, representing the rate of weight loss. The initial weight loss was observed between 50 °C and 130 °C, which was related to the release of water from the samples [52]. More interestingly, the first maximum mass loss rates were observed in the BBG, LBG, and WBG samples at temperatures of 75.7 °C, 84.6 °C, and 75.4 °C, respectively, revealing that LBG had the strongest water-binding capacity. In a previous study, it was also reported that the stable weight loss of  $\beta$ -glucan at high temperatures (<200 °C) was caused by non-covalent bond breaking [53]. Meanwhile, the significant weight loss occurring in the 180–350 °C range was attributed to the decomposition of  $\beta$ -glucan. The shapes of the DTG curves for BBG, LBG, and WBG exhibited narrow peaks, indicating that all the samples had a more uniform molecular weight distribution [31]. As expected, the pyrolysis temperatures of the three BG samples almost overlapped, suggesting that there was little difference in the molecular structure among the different colored samples. Specifically, as illustrated in Figure 9B, the highest pyrolysis temperature was found in LBG (303.3 °C) followed by WBG (301.9 °C) and BBG (301.7 °C).

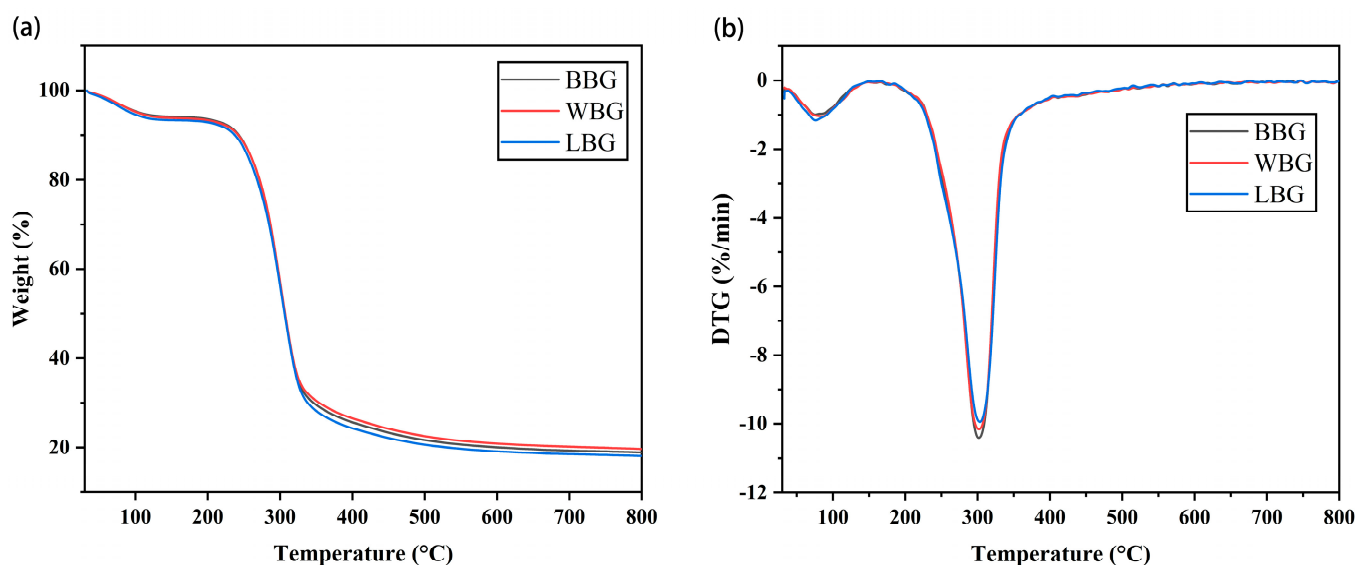


**Figure 10.** TG (a) and DTG (b) curves of BBG, LBG, WBG (BBG indicates black highland barley  $\beta$ -glucan; LBG indicates blue highland barley  $\beta$ -glucan; WBG indicates white highland barley  $\beta$ -glucan).

## 4. Conclusions

Our present work showed that HB  $\beta$ -glucan mainly comprised glucose, regardless of the color. However, there were still many differences in the molecular structure parameters of the BBG, LBG, and WBG samples. 4-Glc(p), 3-Glc(p), and t-Glc(p) accounted for a larger proportion (>90%) of the total methylated residues. Additionally, there was no 3,4-Glc(p) in LBG. The  $M_w$  values of  $\beta$ -glucan extracted from the different colored HB varieties were in the following order: WBG > LBG > BBG, which resulted in different physicochemical properties for BBG, LBG, and WBG. Specifically, LBG presented the best dispersion in water and the highest pyrolysis temperature. Meanwhile, WBG and LBG samples, with large

molecular weight, showed a higher shear viscosity than the BBG sample. Interestingly, the  $G'$  value of the BBG fluids was lower than the  $G''$  value, which is a typical characteristic of entangled viscoelastic liquids. In summary, the gel-like properties of high-molecular-weight  $\beta$ -glucan suggest potential applications in food processing, cosmetics, and drug delivery.

**Supplementary Materials:** The following supporting information can be downloaded at <https://www.mdpi.com/article/10.3390/foods14020316/s1>.

**Author Contributions:** Conceptualization, W.G.; Methodology, B.C.; Software, P.Y.; Formal analysis, Z.W. and Y.C.; Investigation, P.Y., X.K. and P.L.; Data curation, P.L.; Writing—original draft, P.Y.; Writing—review & editing, B.C.; Visualization, P.Y.; Supervision, Z.W. and W.G.; Project administration, X.K.; Funding acquisition, B.C. and W.G. All authors have read and agreed to the published version of the manuscript.

**Funding:** This research was funded by Central Guided Local Science and Technology Development Fund Project (YDZX2022150), Special Funds for Taishan Scholars Project (No. ts201712060), Talent Funds of Science, Education and Industry of Qilu University of Technology (Shandong Academy of Sciences) (2023RCKY242), Major Innovation Pilot Project of Integration of Science, Education and Industry of Qilu University of Technology (Shandong Academy of Sciences) (2022JBZ01-08, 2024ZDZX05), and Innovative Teaching Team of Qilu University of Technology (2024cxjxt03).

**Institutional Review Board Statement:** Not applicable.

**Informed Consent Statement:** Not applicable.

**Data Availability Statement:** The original contributions presented in this study are included in the article/Supplementary Materials. Further inquiries can be directed to the corresponding authors.

**Conflicts of Interest:** The authors declare no conflicts of interest.

## References

1. Subramanian, H.; Krishnan, M.; Mahalingam, A. Photocatalytic dye degradation and photoexcited anti-microbial activities of green zinc oxide nanoparticles synthesized via Sargassum muticum extracts. *RSC Adv.* **2022**, *12*, 985–997. [CrossRef]
2. Sujithra, S.; Arthanareeswaran, G.; Ismail, A.F.; Taweepreda, W. Isolation, purification and characterization of  $\beta$ -glucan from cereals—a review. *Int. J. Biol. Macromol.* **2024**, *256*, 128255. [CrossRef] [PubMed]
3. Henrion, M.; Francey, C.; Lê, K.A.; Lamothe, L. Cereal B-glucans: The impact of processing and how it affects physiological responses. *Nutrients* **2019**, *11*, 1729. [CrossRef] [PubMed]
4. Maheshwari, G.; Sowrirajan, S.; Joseph, B. Extraction and isolation of  $\beta$ -glucan from grain sources—A review. *J. Food Sci.* **2017**, *82*, 1535–1545. [CrossRef] [PubMed]
5. Martínez-Subirà, M.; Romero, M.P.; Puig, E.; Macià, A.; Romagosa, I.; Moralejo, M. Purple, high  $\beta$ -glucan, hullless barley as valuable ingredient for functional food. *LWT-Food. Sci. Technol.* **2020**, *131*, 109582. [CrossRef]
6. Izydorczyk, M.S.; Macri, L.J.; MacGregor, A.W. Structure and physicochemical properties of barley non-starch polysaccharides—I. Water-extractable  $\beta$ -glucans and arabinoxylans. *Carbohydr. Polym.* **1998**, *35*, 249–258. [CrossRef]
7. Manthey, F.A.; Hareland, G.A.; Huseby, D.J. Soluble and insoluble dietary fiber content and composition in oat. *Cereal Chem.* **1999**, *76*, 417–420. [CrossRef]
8. Ji, X.L.; Cheng, Y.Q.; Tian, J.Y.; Zhang, S.Q.; Jing, Y.S.; Shi, M.M. Structural characterization of polysaccharide from jujube (*Ziziphus jujuba* Mill.) fruit. *Chem. Biol. Technol. Agric.* **2021**, *8*, 1–7. [CrossRef]
9. Rahar, S.; Swami, G.; Nagpal, N.; Nagpal, M.A.; Singh, G.S. Preparation, characterization, and biological properties of  $\beta$ -glucans. *J. Adv. Pharm. Technol. Res.* **2011**, *2*, 94–103. [CrossRef]
10. Ji, X.L.; Guo, J.H.; Tian, J.Y.; Ma, K.; Liu, Y.Q. Research progress on degradation methods and product properties of plant polysaccharides. *J. Light Ind.* **2023**, *38*, 55–62.
11. Yuan, C.; Hu, R.; He, L.; Hu, J.; Liu, H. Extraction and prebiotic potential of  $\beta$ -glucan from highland barley and its application in probiotic microcapsules. *Food Hydrocoll.* **2023**, *139*, 108520. [CrossRef]
12. Cao, H.; Li, R.; Shi, M.; Song, H.; Li, S.; Guan, X. Promising effects of  $\beta$ -glucans on gelation in protein-based products: A review. *Int. J. Biol. Macromol.* **2023**, *256*, 127574. [CrossRef] [PubMed]
13. Szpicer, A.; Onopiuk, A.; Półtorak, A.; Wierzbicka, A. Influence of oat  $\beta$ -glucan and canola oil addition on the physico-chemical properties of low-fat beef burgers. *J. Food Process. Preserv.* **2018**, *42*, e13785. [CrossRef]

14. Li, J.; Zhang, X.; Zhou, W.J.; Tu, Z.X.; Yang, S.; Xia, T.L.; Chen, Z.X.; Du, Y. Intelligent films based on highland barley  $\beta$ -glucan/highland barley prolamin incorporated with black rice bran anthocyanins. *Food Packag. Shelf* **2023**, *39*, 101146. [[CrossRef](#)]
15. Yuan, T.; Zhao, S.; Yang, J.; Niu, M.; Xu, Y. Structural characteristics of  $\beta$ -glucans from various sources and their influences on the short-and long-term starch retrogradation in wheat flour. *Int. J. Biol. Macromol.* **2024**, *264*, 130561. [[CrossRef](#)] [[PubMed](#)]
16. Obadi, M.; Sun, J.; Xu, B. Highland barley: Chemical composition, bioactive compounds, health effects, and applications. *Food Res. Int.* **2021**, *140*, 110065. [[CrossRef](#)]
17. Li, Y.; You, M.L.; Liu, H.B.; Liu, X. Comparison of distribution and physicochemical properties of  $\beta$ -glucan extracted from different fractions of highland barley grains. *Int. J. Biol. Macromol.* **2021**, *189*, 91–99. [[CrossRef](#)]
18. Wang, C.; Tian, X.Y.; Fang, S.J.; Ren, C.J.; Huang, C.S.; Yuan, G.Q.; Zeng, X.X. Brewing characteristics, physicochemical constituents, and antioxidant activity of the infusions of colored highland barley roasted at different times. *J. Cereal Sci.* **2023**, *110*, 103639. [[CrossRef](#)]
19. Bai, Y.P.; Zhou, H.M.; Zhu, K.R.; Li, Q. Effect of thermal processing on the molecular, structural, and antioxidant characteristics of highland barley  $\beta$ -glucan. *Carbohydr. Polym.* **2021**, *271*, 118416. [[CrossRef](#)]
20. Kupetz, M.; Sacher, B.; Becker, T. Impact of flavouring substances on the aggregation behaviour of dissolved barley  $\beta$ -glucans in a model beer. *Carbohydr. Polym.* **2016**, *143*, 204–211. [[CrossRef](#)]
21. Gao, W.; Zhu, J.; Kang, X.M.; Wang, B.; Liu, P.F.; Cui, B.; Abd El-Aty, A.M. Development and characterization of starch films prepared by extrusion blowing: The synergistic plasticizing effect of water and glycerol. *LWT-Food. Sci. Technol.* **2021**, *148*, 111820. [[CrossRef](#)]
22. Li, L.Y.; Wang, Y.X.; Zhang, T.; Zhang, J.F.; Pan, M.; Huang, X.J.; Yin, J.Y.; Nie, S.P. Structural characteristics and rheological properties of alkali-extracted arabinoxylan from dehulled barley kernel. *Carbohydr. Polym.* **2020**, *249*, 116813. [[CrossRef](#)] [[PubMed](#)]
23. Du, B.; Nie, S.P.; Peng, F.; Yang, Y.D.; Xu, B.J. A narrative review on conformational structure characterization of natural polysaccharides. *Food Front.* **2022**, *3*, 631–640. [[CrossRef](#)]
24. Gao, W.; Zhu, J.; Liu, P.F.; Cui, B.; Abd El-Aty, A.M. Preparation and characterization of octenyl succinylated starch microgels via a water-in-oil (W/O) inverse microemulsion process for loading and releasing epigallocatechin gallate. *Food Chem.* **2021**, *355*, 129661. [[CrossRef](#)] [[PubMed](#)]
25. Karimi, R.; Azizi, M.H.; Xu, Q. Effect of different enzymatic extractions on molecular weight distribution, rheological and microstructural properties of barley bran  $\beta$ -glucan. *Int. J. Biol. Macromol.* **2019**, *126*, 298–309. [[CrossRef](#)]
26. Gao, W.; Sui, J.; Yu, B.; Liu, P.F.; Cui, B. Effect of shell separation pretreatment on the physicochemical properties of octenyl succinic anhydride-modified starch. *Int. J. Biol. Macromol.* **2022**, *221*, 1–7. [[CrossRef](#)]
27. Iqbal, S.; Wu, P.; Kirk, T.V.; Chen, X.D. Amylose content modulates maize starch hydrolysis, rheology, and microstructure during simulated gastrointestinal digestion. *Food Hydrocoll.* **2021**, *110*, 106171. [[CrossRef](#)]
28. Ma, H.; Huang, Q.; Ren, J.; Zheng, Z.; Xiao, Y. Structure characteristics, solution properties and morphology of oxidized yeast  $\beta$ -glucans derived from controlled TEMPO-mediated oxidation. *Carbohydr. Polym.* **2020**, *250*, 116924. [[CrossRef](#)]
29. Xu, S.; Xu, X.; Zhang, L. Effect of heating on chain conformation of branched  $\beta$ -glucan in water. *J. Phys. Chem. B* **2013**, *117*, 8370–8377. [[CrossRef](#)] [[PubMed](#)]
30. Jian, W.J.; Tu, L.Y.; Wu, L.L.; Xiong, H.J.; Pang, J.; Sun, Y.M. Physicochemical properties and cellular protection against oxidation of degraded Konjac glucomannan prepared by  $\gamma$ -irradiation. *Food Chem.* **2017**, *231*, 42–50. [[CrossRef](#)]
31. Zhao, Y.; Zhou, H.M.; Huang, Z.H.; Zhao, R.Y. Different aggregation states of barley  $\beta$ -glucan molecules affects their solution behavior: A comparative analysis. *Food Hydrocoll.* **2020**, *101*, 105543. [[CrossRef](#)]
32. Li, Q.; Liu, J.; Zhai, H.S.; Zhang, Z.H.; Xie, R.; Xiao, F.T.; Zeng, X.Q.; Zhang, Y.H.; Li, Z.Y.; Pan, Z.F. Extraction and characterization of waxy and normal barley  $\beta$ -glucans and their effects on waxy and normal barley starch pasting and degradation properties and mash filtration rate. *Carbohydr. Polym.* **2023**, *302*, 120405. [[CrossRef](#)] [[PubMed](#)]
33. Cai, G.F.; Wu, C.H.; Zhu, T.Y.; Peng, S.; Xu, S.W.; Hu, Y.L.; Liu, Z.G.; Yang, Y.; Wang, D.Y. Structure of a Pueraria root polysaccharide and its immunoregulatory activity on T and B lymphocytes, macrophages, and immunosuppressive mice. *Int. J. Biol. Macromol.* **2023**, *230*, 123386. [[CrossRef](#)]
34. Pérez-Bassart, Z.; Falcó, I.; Martínez-Sanz, M.; Martínez-Abad, A.; Sánchez, G.; López-Rubio, A.; Fabra, M.J. Antiviral and technological properties of  $\beta$ -glucan-rich aqueous fractions from *Pleurotus ostreatus* waste biomass. *Food Hydrocoll.* **2024**, *146*, 109308. [[CrossRef](#)]
35. Gao, W.; Dong, H.Z.; Hou, H.X.; Zhang, H. Effects of clays with various hydrophilicities on properties of starch-clay nanocomposites by film blowing. *Carbohydr. Polym.* **2012**, *88*, 321–328. [[CrossRef](#)]
36. Liu, H.B.; Li, Y.; You, M.L.; Liu, X. Comparison of physicochemical properties of  $\beta$ -glucans extracted from hull-less barley bran by different methods. *Int. J. Biol. Macromol.* **2021**, *182*, 1192–1199. [[CrossRef](#)]
37. Dong, J.L.; Yang, M.; Zhu, Y.Y.; Shen, R.L.; Zhang, K.Y. Comparative study of thermal processing on the physicochemical properties and prebiotic effects of the oat  $\beta$ -glucan by in vitro human fecal microbiota fermentation. *Food Res. Int.* **2020**, *138*, 109818. [[CrossRef](#)] [[PubMed](#)]

38. Ahmad, M.; Gani, A.; Shah, A.; Gani, A.; Masoodi, F.A. Germination and microwave processing of barley (*Hordeum vulgare* L.) changes the structural and physicochemical properties of  $\beta$ -d-glucan & enhances its antioxidant potential. *Carbohydr. Polym.* **2016**, *153*, 696–702. [[PubMed](#)]
39. Guo, R.; Xu, Z.X.; Wu, S.F.; Li, X.J.; Li, J.N.; Hu, H.; Wu, Y.; Ai, L. Molecular properties and structural characterization of an alkaline extractable arabinoxylan from hull-less barley bran. *Carbohydr. Polym.* **2019**, *218*, 250–260. [[CrossRef](#)]
40. Shah, A.; Masoodi, F.A.; Gani, A.; Ashwar, B.A. Effect of  $\gamma$ -irradiation on antioxidant and antiproliferative properties of oat  $\beta$ -glucan. *Radiat. Phys. Chem.* **2015**, *117*, 120–127. [[CrossRef](#)]
41. Cory, A.T.; Gangola, M.P.; Anyia, A.; Båga, M.; Chibbar, R.N. Genotype, environment and G  $\times$  E interaction influence (1, 3; 1, 4)- $\beta$ -d-glucan fine structure in barley (*Hordeum vulgare* L.). *J. Sci. Food Agric.* **2017**, *97*, 743–752. [[CrossRef](#)]
42. Ma, X.; Dong, L.; He, Y.; Chen, S.W. Effects of ultrasound-assisted H<sub>2</sub>O<sub>2</sub> on the solubilization and antioxidant activity of yeast  $\beta$ -glucan. *Ultrason. Sonochem.* **2022**, *90*, 106210. [[CrossRef](#)] [[PubMed](#)]
43. Shaheen, T.I.; Hussien, G.M.A.; Mekawey, A.A.; Ghalia, H.H.A.; Youssry, A.A.; El Mokadem, M.T. Facile extraction of nanosized  $\beta$ -glucans from edible mushrooms and their antitumor activities. *J. Food Compos. Anal.* **2022**, *111*, 104607. [[CrossRef](#)]
44. Gong, J.J.; Su, Y.; Lei, J.N.; Zhu, S.; He, Y.; Tan, C.P.; Liu, Y.F.; Xu, Y.J. Construction and characterization of pickering emulsion gels stabilized by  $\beta$ -glucans microgel particles. *Food Hydrocoll.* **2024**, *151*, 109778. [[CrossRef](#)]
45. Singh, H.; Sodhi, N.S.; Singh, N. Characterisation of starches separated from sorghum cultivars grown in India. *Food Chem.* **2010**, *119*, 95–100. [[CrossRef](#)]
46. Yang, X.; Feng, M.Q.; Sun, J.; Xu, X.L.; Zhou, G.H. The influence of flaxseed gum on the retrogradation of maize starch. *Int. J. Food Sci. Technol.* **2017**, *52*, 2654–2660. [[CrossRef](#)]
47. Oyeyinka, S.A.; Singh, S.; Amonsou, E.O. Physicochemical properties of starches extracted from bambara groundnut landraces. *Starch-Stärke* **2017**, *69*, 1600089. [[CrossRef](#)]
48. Ma, Y.S.; Pan, Y.; Xie, Q.T.; Li, X.M.; Zhang, B.; Chen, H.Q. Evaluation studies on effects of pectin with different concentrations on the pasting, rheological and digestibility properties of corn starch. *Food Chem.* **2019**, *274*, 319–323. [[CrossRef](#)]
49. Li, Y.; Shabani, K.I.; Liu, H.; Guo, Q.; Liu, X. Structural, physicochemical and rheological properties of a novel native starch obtained from *Rhizoma Gastrodiae*. *Food Struct.* **2020**, *25*, 100148. [[CrossRef](#)]
50. Aktas-Akyildiz, E.; Sibakov, J.; Nappa, M.; Hytonen, E.; Koksel, H.; Poutanen, K. Extraction of soluble beta-glucan from oat and barley fractions: Process efficiency and dispersion stability. *J. Cereal Sci.* **2018**, *81*, 60–68. [[CrossRef](#)]
51. Tangsrianugul, N.; Wongsagonsup, R.; Suphantharika, M. Physicochemical and rheological properties of flour and starch from Thai pigmented rice cultivars. *Int. J. Biol. Macromol.* **2019**, *137*, 666–675. [[CrossRef](#)]
52. Janković, B. Thermal characterization and detailed kinetic analysis of Cassava starch thermo-oxidative degradation. *Carbohydr. Polym.* **2013**, *95*, 621–629. [[CrossRef](#)] [[PubMed](#)]
53. Xu, S.; Xu, X.; Zhang, L. Branching structure and chain conformation of water-soluble glucan extracted from *Auricularia auricula-judae*. *J. Agric. Food Chem.* **2012**, *60*, 3498–3506. [[CrossRef](#)]

**Disclaimer/Publisher’s Note:** The statements, opinions and data contained in all publications are solely those of the individual author(s) and contributor(s) and not of MDPI and/or the editor(s). MDPI and/or the editor(s) disclaim responsibility for any injury to people or property resulting from any ideas, methods, instructions or products referred to in the content.